bioRxiv preprint doi: https://doi.org/10.1101/2020.03.06.979542; this version posted March 8, 2020. The copyright holder for this preprint (which was not certified by peer review) is the author/funder, who has granted bioRxiv a license to display the preprint in perpetuity. It is made available under aCC-BY-NC-ND 4.0 International license.

"Human *METTL7B* Encodes an Alkyl Thiol Methyltransferase that Methylates Hydrogen Sulfide"

Benjamin J. Maldonato and Dr. Rheem A. Totah

University of Washington

Department of Medicinal Chemistry

1959 NE Pacific Ave,

Box 357610

Seattle, WA 98195

Corresponding Author: Dr. Rheem A. Totah

Email: rtotah@uw.edu

Phone: 206-543-9481

bioRxiv preprint doi: https://doi.org/10.1101/2020.03.06.979542; this version posted March 8, 2020. The copyright holder for this preprint (which was not certified by peer review) is the author/funder, who has granted bioRxiv a license to display the preprint in perpetuity. It is made available under aCC-BY-NC-ND 4.0 International license.

Summary Paragraph/Abstract:

Methyltransferase-like protein 7B (METTL7B) is implicated in tumor growth and progression while gene expression is upregulated in several different disease states such as rheumatoid arthritis and breast cancer. Yet, the catalytic function of METTL7B has not been characterized. Here we demonstrate that *METTL7B* encodes a protein that catalyzes the transfer of a methyl group from S-adenosyl-L-methionine (SAM) to hydrogen sulfide (H_2S) to form methanethiol (CH_3SH). Several exogenous aliphatic thiols were also identified as substrates. Modulation of *METTL7B* gene expression in HepG2 and HeLa cell culture directly alters the methylation of captopril, a marker reaction of alkyl thiol methyltransferase (TMT) activity(1, 2). Furthermore, cloned and recombinantly expressed and purified METTL7B full length protein methylates several thiol compounds, including hydrogen sulfide, 7α-thiospironolactone, captopril, and L-penicillamine in a concentration dependent manner. Endogenous thiols such as glutathione and cysteine or classic probe substrates of other known small molecule *S*-, *N*-, and *O*-methyltransferases were not substrates for METTL7B. Our results unequivocally demonstrate, and for the first time, that METTL7B, a protein implicated in several disease states, is an alkyl thiol methyltransferase(3–5). Identifying the catalytic function of METTL7B will enable future pharmacological research in disease pathophysiology where *METTL7B* expression and H_2S levels can potentially alter the redox state and growth cycle of cells.

Introduction:

Hydrogen sulfide (H_2S) is a gasotransmitter that regulates inflammatory and cell cycle processes(6). It is biosynthesized by three different enzymes, cystathionine γ-lyase (CSE), cystathionine ß-synthase (CBS), and 3-mercaptopyruvate sulfurtransferase (3-MST)(7). CBS

bioRxiv preprint doi: https://doi.org/10.1101/2020.03.06.979542; this version posted March 8, 2020. The copyright holder for this preprint (which was not certified by peer review) is the author/funder, who has granted bioRxiv a license to display the preprint in perpetuity. It is made available under aCC-BY-NC-ND 4.0 International license.

activity is inhibited by carbon monoxide and nitric oxide but is activated by S-adenosyl-L-methionine (SAM)(8, 9). Therefore, production of hydrogen sulfide is sensitive to intracellular redox state. Once formed, hydrogen sulfide causes physiological effects by formation of persulfide bonds to protein cysteine residues(10). Catabolism of hydrogen sulfide is believed to be primarily driven by oxidation(11). This route of metabolism may be less prominent in organs outside of the gut and under hypoxic conditions, such as in the interior of solid tumors(12, 13). In these instances, methylation can play a key role in hydrogen sulfide catabolism yet little is known about this process or the enzyme that catalyzes this reaction. In this report, we identify METTL7B as an alkyl thiol methyltransferase that catalyzes the transfer of a methyl group from S-adenosyl-L-methionine (SAM) to hydrogen sulfide and several aliphatic thiol-containing compounds.

To date, the catalytic function of methyltransferase-like protein 7B (METTL7B) was unknown despite being implicated in several disease states. Specifically, *METTL7B* gene expression is significantly altered in kidney disease, acute respiratory distress syndrome, and numerous cancers, including breast, non-small cell lung, thyroid, and ovarian(3–5, 14–17). METTL7B expression appears to be responsive to inflammation signaling pathways via JAK1(18, 19). Gene expression also changes with respect to cellular redox state and is associated with individual response to certain chemotherapeutics(20, 21). In non-small cell lung cancer, *METTL7B* contributes to tumorigenesis and progression by regulating cell cycle progression. Gene silencing reduced tumor growth and progression both *in vitro* and *in vivo* suggesting METTL7B as a potential therapeutic target(17).

Interest in METTL7B originated as we were attempting to identify the elusive alkyl thiol methyltransferase (TMT) responsible for the methylation of the active metabolite of clopidogrel

bioRxiv preprint doi: https://doi.org/10.1101/2020.03.06.979542; this version posted March 8, 2020. The copyright holder for this preprint (which was not certified by peer review) is the author/funder, who has granted bioRxiv a license to display the preprint in perpetuity. It is made available under aCC-BY-NC-ND 4.0 International license.

in vivo(22). This microsomal enzyme catalyzes the methylation of aliphatic thiols in humans, including hydrogen sulfide, captopril, 7α-thiospironolactone, D- and L-penicillamine, and the active metabolites of prasugrel, and ziprasidone(1, 2, 23–27). However, despite numerous attempts, researchers have not successfully identified the TMT gene or protein (28–31).

Our preliminary approach to identify TMT expanded on earlier research which attempted to purify TMT from rat liver microsomes using a number of chromatographic steps(28, 31). After significant increases in TMT specific activity, preliminary non-targeted proteomic experiments were conducted to identify potential methyltransferase proteins in the TMT-active fractions. The major candidate protein in active fractions was identified as rat METTL7B which was also localized to the endoplasmic reticulum (Extended Data Table 1). Rat and human METTL7B share 83% sequence homology, which suggests a conserved function. Subsequent experiments modulating the expression of human METTL7B in two cell lines also altered captopril methylation, a known TMT substrate. Once identified, we cloned, recombinantly expressed, and purified human full length METTL7B in *E. coli* and conducted small molecule substrate screening with the purified protein. The activity screens confirmed that METTL7B specifically catalyzes SAM-dependent methylation of aliphatic thiol compounds, including hydrogen sulfide, in a time and protein concentration dependent manner. No methylation was observed with classic probe substrates of other known small molecule *S*-, *N*-, and *O*-methyltransferases(32–36) or endogenous thiols such as cysteine or glutathione.

bioRxiv preprint doi: https://doi.org/10.1101/2020.03.06.979542; this version posted March 8, 2020. The copyright holder for this preprint (which was not certified by peer review) is the author/funder, who has granted bioRxiv a license to display the preprint in perpetuity. It is made available under aCC-BY-NC-ND 4.0 International license.

Results:

METTL7B Gene Expression Modulation in Mammalian Cell Culture:

Treating HepG2 cells with *METTL7B* specific small interfering RNA (siRNA) caused an average of 60% decrease in *METTL7B* mRNA expression compared to cells treated with a scrambled negative siRNA control (Figure 1A). Incubation with captopril following siRNA treatment, a previously reported TMT- probe substrate, showed an average 51% decrease in captopril methylation in HepG2 cells with reduced *METTL7B* gene expression (Figure 1B).

METTL7B gene expression increased over 1,000-fold in HeLa cells treated with a constitutive overexpression plasmid containing the *METTL7B* gene sequence compared to cells treated with an empty control plasmid as measured by RT-PCR (Figure 1C). Captopril methylation subsequently increased 10-fold in cells overexpressing *METTL7B* compared to control cells (Figure 1D). Cells transfected with the METTL7B overexpression plasmid show

bioRxiv preprint doi: https://doi.org/10.1101/2020.03.06.979542; this version posted March 8, 2020. The copyright holder for this preprint (which was not certified by peer review) is the author/funder, who has granted bioRxiv a license to display the preprint in perpetuity. It is made available under aCC-BY-NC-ND 4.0 International license.

formation of FLAG-tagged METTL7B (Lane 2, Figure 1E) compared to cells treated with an empty overexpression plasmid (Lane 1, Figure 1F).

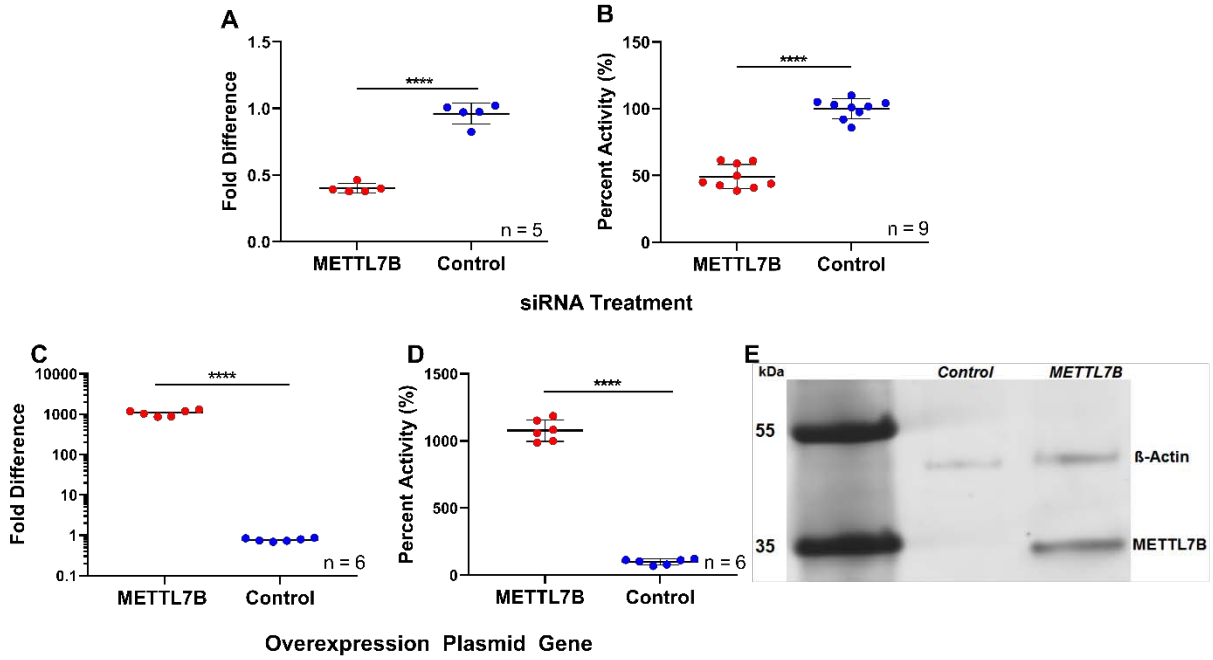

Figure 1. Alteration of *METTL7B* gene expression in human cell culture: A) *METTL7B* gene expression significantly decreased in HepG2 cells compared to controls when treated with anti-*METTL7B* siRNA for 72 hours. **B)** Methylation of captopril activity significantly decreased in HepG2 cells treated with *METTL7B* siRNA compared to control cells. **C)** HeLa cells treated with a *METTL7B* overexpression plasmid showed ~ 1,000-fold increase in *METT7B* gene expression compared to control cells transfected with an empty expression vector. **D)** HeLa cells transfected with the *METTL7B* expression vector showed a 10-fold increase in captopril methylation activity compared to negative control cells. **E)** FLAG-tagged METTL7B expression is only observed in cells treated with the *METTL7B* overexpression plasmid compared to controls (Lanes 2 and 1 respectively). ß-actin was used as a loading control. All data is presented as the mean ± standard deviation. Individual data points from two (A, C, and D) or three (B) experiments are plotted. Significance was determined using unpaired two-tailed *t* test. ****P<0.0001.

bioRxiv preprint doi: https://doi.org/10.1101/2020.03.06.979542; this version posted March 8, 2020. The copyright holder for this preprint (which was not certified by peer review) is the author/funder, who has granted bioRxiv a license to display the preprint in perpetuity. It is made available under aCC-BY-NC-ND 4.0 International license.

Expression and Purification of METTL7B Fusion Protein:

The full-length *METTL7B* gene sequence was inserted into a pET21 expression plasmid to express a unique fusion protein in *E. coli*. The fusion protein, henceforth referred to as pET21 METTL7B, is 57.5 kDa and contains a dual His-GST affinity/solubilization tag coupled to the N-terminus of the native METTL7B protein. We developed a dual-stage affinity purification protocol as detailed in the Methods section. The resulting purified protein fraction predominantly contains the pET21 METTL7B fusion protein construct. The fusion protein band is indicated in Figure 2 by the letter "A". pET21 METTL7B was also identified by proteomics in both the purified protein fraction, and in the 55 kDa band in lane 1 of Figure 2 (Extended Data Tables 2 and 3). The lower bands around 30-35 kDa were determined by western blot to be co-purified affinity tag GST protein without METTL7B, as indicated by "B" and "C" in Figure 2. Tryptic digest showed that the remaining background bands are co-purified *E. coli* proteins (Extended Data Table 4).

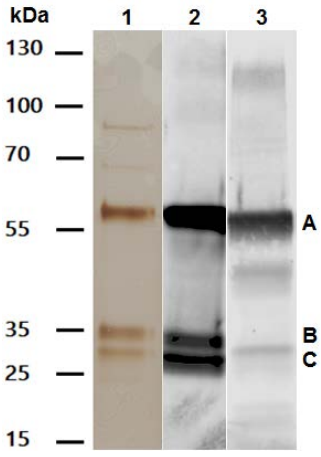

Figure 2. Analysis of purified pET21 METTL7B: Lane 1) SDS-PAGE silver stain of a representative gel showing purified pET21 METTL7B. The gel was loaded with a total of 1 µg total protein as determined by A_{280}. **Lane 2)** anti-GST western blot of purified pET21 METTL7B. The gel was loaded with a total of 0.1 µg total protein. **Lane 3)** anti-METTL7B western blot of purified pET21 METTL7B. The gel was loaded with 0.1 µg total protein. Molecular weight markers from the PageRuler Plus Prestained Protein Ladder are shown on the left. The pET21 METTL7B band is marked by the letter A. The lower molecular bands, marked by letters B and C, are fusion protein fragments containing the dual His-GST affinity tag.

bioRxiv preprint doi: https://doi.org/10.1101/2020.03.06.979542; this version posted March 8, 2020. The copyright holder for this preprint (which was not certified by peer review) is the author/funder, who has granted bioRxiv a license to display the preprint in perpetuity. It is made available under aCC-BY-NC-ND 4.0 International license.

Substrate Specificity Testing and Kinetic Analysis of pET21 METTL7B:

A number of known methyltransferase substrates as well as endogenous thiol compounds were screened for methylation using recombinant pET21 METTL7B. Substrates were screened at concentrations at least three times higher than previously reported K_m values to ensure detection of methylation activity. We accounted for non-enzymatic methylation, which has been reported for some potential substrates, by including boiled enzyme and buffer-only controls and subtracting that turnover from the experimental samples. Qualitative screening results are presented below in Table 1. A subset of the semi-quantitative screening results is shown in Extended Data Figure 1. Only aliphatic thiol compounds show significant methylation signal above baseline.

Table 1: Relative Turnover of Probe Substrates with METTL7B

Substrate	**Activity**	**Non-Substrate**	**Activity**
7α-thiospironolactone	+++	Dopamine	-
Dithiothreitol	+++	Phenylethanolamine	-
Thioglucose	++	Histamine	-
L-penicillamine	++	6-mercaptopurine	-
D-penicillamine	++	N-acetylcysteine	-
Hydrogen Sulfide	++	Arsenic Trioxide	-
Captopril	+	Cantharidin	-
Prasugrel Active Metabolite	+	Coenzyme M	-
		Cysteine	-
		Glutathione	-

We determined kinetic parameters for a subset of the identified substrates and they are presented below in Figure 3. All substrates were only methylated in the presence of SAM and catalytic activity was saturable and can be destroyed upon pre-boiling the enzyme. Additionally, kinetic experiments were conducted under conditions where methylation was linear with respect to incubation time and protein concentration (Extended Data Figures 2 and 3).

bioRxiv preprint doi: https://doi.org/10.1101/2020.03.06.979542; this version posted March 8, 2020. The copyright holder for this preprint (which was not certified by peer review) is the author/funder, who has granted bioRxiv a license to display the preprint in perpetuity. It is made available under aCC-BY-NC-ND 4.0 International license.

Hydrogen sulfide and SAM kinetic curves were obtained using mass spectrometric methods measuring formation of methanethiol and *S*-methyl captopril respectively. 7α-thiospironolactone and dithiothreitol kinetic curves were obtained using the MTaseGlo kit (Promega) which measures the formation of S-adenosyl-L-homocysteine (SAH), the byproduct of all SAM-dependent methylation reactions.

Most substrates exhibit mid- to low-micromolar affinities to pET21 METTL7B. All substrates display classic Michaelis-Menten kinetics as evidenced by highly linear Eadie-Hofstee transformations of the data (Extended Data Figure 4).

Figure 3. Rate of thiol methyl formation for pET21 METTL7B with multiple probe substrates: A) Luminescence vs concentration curves for 7α-thiospironolactone methylation as measured by SAH formation. **B)** Luminescence vs concentration curve for dithiothreitol methylation as measured by SAH formation. **C)** Peak area ratio (PAR) vs concentration curve for S-adenosyl-L-methionine use as measured by captopril methylation. **D)** PAR vs concentration curve for hydrogen sulfide methylation as measured by formation of methanethiol. All data is presented as the mean ± standard deviation of biological replicates.

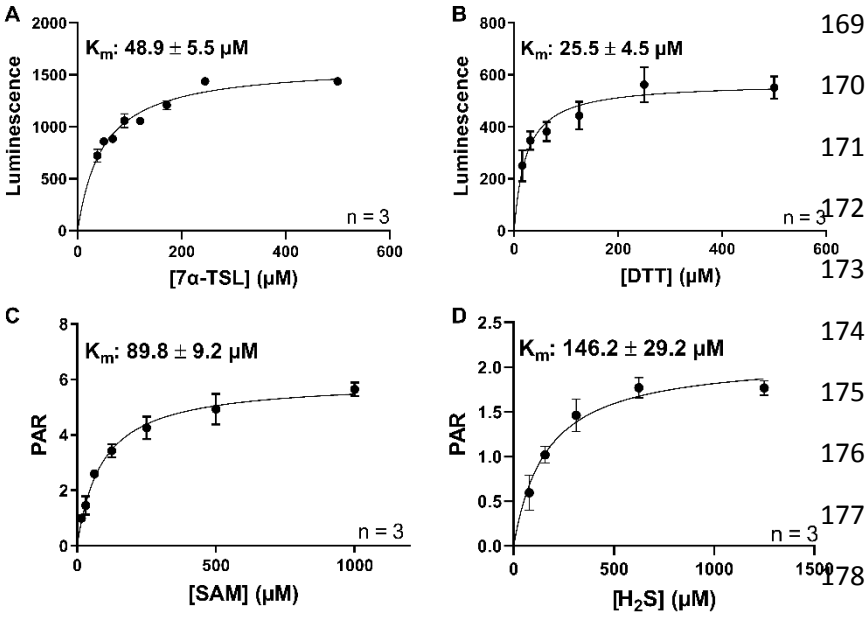

bioRxiv preprint doi: https://doi.org/10.1101/2020.03.06.979542; this version posted March 8, 2020. The copyright holder for this preprint (which was not certified by peer review) is the author/funder, who has granted bioRxiv a license to display the preprint in perpetuity. It is made available under aCC-BY-NC-ND 4.0 International license.

Discussion:

The key finding in this paper is the METTL7B encodes for an alkyl thiol methyltransferase. We originally identified METTL7B as a candidate alkyl thiol methyltransferase by proteomic analysis of partially purified rat liver microsomes. Subsequent bioinformatics analysis determined that the human METTL7B had high sequence identity with the rat enzyme and has a putative SAM binding domain. We first manipulated *METTL7B* gene expression in human cell culture models to test that the gene product was associated with TMT activity using captopril as a probe substrate. We chose HepG2 and HeLa cells for gene knockdown and overexpression experiments because of their respectively high and low basal levels of *METTL7B* mRNA. Reduction of *METTL7B* gene, and protein, expression resulted in a decrease in captopril methylation. The opposite trend was observed upon gene overexpression, where increasing *METTL7B* gene and protein expression vastly increased captopril methylation.

We then designed a plasmid to express and purify recombinant full-length METTL7B to confirm that it was catalyzing the methylation event unequivocally. In our study, we discovered that glycerol greatly stabilized recombinant METTL7B in solution and that methylation activity was enhanced by adding dimyristoyl-*sn*-glycero-3-PG (DMPG) liposomes to reconstitute the protein. This was critical to maintain activity of an enzyme that is highly unstable which may have contributed to lack of characterization to date.

The METTL7B fusion protein catalyzes the *S*-methylation of multiple previously identified TMT-specific substrates in a SAM-dependent manner. We observed no methylation with a variety of probe substrates for other small molecule methyltransferases, as shown in Figure 3. The substrates that undergo methylation conform to the substrate specificity

bioRxiv preprint doi: https://doi.org/10.1101/2020.03.06.979542; this version posted March 8, 2020. The copyright holder for this preprint (which was not certified by peer review) is the author/funder, who has granted bioRxiv a license to display the preprint in perpetuity. It is made available under aCC-BY-NC-ND 4.0 International license.

parameters previously determined using liver microsomes(1, 2, 24, 26). In general, METTL7B methylates compounds that contain an easily accessible aliphatic thiol functional group. It is important to note that METTL7B does not methylate 6-mercaptopurine, a classic thiopurine methyltransferase (TPMT) probe substrate(37). This further confirms that METTL7B catalyzes TMT-specific reactions rather than TPMT reactions. Additionally, consistent with prior reports, neither cysteine nor glutathione are substrates, but hydrogen sulfide is enzymatically methylated(23).

A potential key endogenous function of METTL7B is that it catalyzes the methylation of hydrogen sulfide to methanethiol which has been detected *in vivo* but the exact function and activity is still unknown. Maintenance of hydrogen sulfide homeostasis is crucial as it is known to play a large role in inflammatory processes, cell cycle, and cancer progression(38). In general, hydrogen sulfide exerts protective effects such as angiogenesis and cell growth at low concentrations. As hydrogen sulfide concentrations increase, its beneficial effects give way to toxicity, resulting in increased apoptosis(39, 40). Therefore, cancer cells with impaired hydrogen sulfide oxidation pathways, due to the hypoxic nature of tumors, likely rely heavily on methylation as a route of catabolism to prevent intracellular H_2S levels from reaching toxic concentrations. Consequently, *METTL7B* is upregulated to potentially increase the rate of clearance of hydrogen sulfide or perhaps to increase formation of methanethiol. It is clear, however, that further research is required to fully characterize the role of METTL7B in the metabolism and homeostasis of hydrogen sulfide, especially in disease states that exhibit altered cellular redox states, such as the hypoxic interior of solid tumors. Additionally, it is important to investigate the role of methanethiol in cancer progression and its potential as a signaling molecule.

bioRxiv preprint doi: https://doi.org/10.1101/2020.03.06.979542; this version posted March 8, 2020. The copyright holder for this preprint (which was not certified by peer review) is the author/funder, who has granted bioRxiv a license to display the preprint in perpetuity. It is made available under aCC-BY-NC-ND 4.0 International license.

Overall, METTL7B possesses all of the known characteristics of the elusive human alkyl thiol methyltransferase (TMT) and should be renamed as alkyl thiol methyltransferase. Human METTL7B clearly catalyzes the SAM-dependent methyl transfer to exogenous and select endogenous thiol compounds, distinct from TPMT and other small molecule methyltransferases. METTL7B is involved in the metabolism of hydrogen sulfide, which may be important in cancer and inflammation where gene expression is highly upregulated and hydrogen sulfide levels are altered. Future work will focus on elucidating the *in vivo* role METTL7B plays in healthy and diseased tissue.

Bibliography:

1. O. H. Drummer, P. Miach, B. Jarrott, S-methylation of captopril. Demonstration of captopril thiol methyltransferase activity in human erythrocytes and enzyme distribution in rat tissues. *Biochem. Pharmacol.* **32**, 1557–62 (1983).

2. R. A. Keith, I. Jardine, A. Kerremans, R. M. Weinshilboum, Human erythrocyte membrane thiol methyltransferase. S-methylation of captopril, N-acetylcysteine, and 7 alpha-thio-spirolactone. *Drug Metab. Dispos.* **12**, 717–24 (1984).

3. H. Liu, Y. Liu, J. Qu, Construction of an eight-gene signature for survival evaluation of papillary thyroid cancer patients. *Int J Clin Exp Med* **12**, 7241–7248 (2019).

4. Z. Dong, *et al.*, Identification of potential key genes in esophagael adenocarcinoma using bioinformatics. *Exp. Ther. Med.* **18**, 3291–3298 (2019).

5. D. Ye, *et al.*, METTL7B promotes migration and invasion in thyroid cancer through epithelial-mesenchymal transition. *J. Mol. Endocrinol.* **63**, 51–61 (2019).

bioRxiv preprint doi: https://doi.org/10.1101/2020.03.06.979542; this version posted March 8, 2020. The copyright holder for this preprint (which was not certified by peer review) is the author/funder, who has granted bioRxiv a license to display the preprint in perpetuity. It is made available under aCC-BY-NC-ND 4.0 International license.

6. F.-F. Guo, T.-C. Yu, J. Hong, J.-Y. Fang, Emerging Roles of Hydrogen Sulfide in Inflammatory and Neoplastic Colonic Diseases . *Front. Physiol.* **7**, 156 (2016).

7. X. Cao, *et al.*, A Review of Hydrogen Sulfide Synthesis, Metabolism, and Measurement: Is Modulation of Hydrogen Sulfide a Novel Therapeutic for Cancer? *Antioxid. Redox Signal.* **31**, 1–38 (2019).

8. K. Módis, *et al.*, Effect of S-adenosyl-l-methionine (SAM), an allosteric activator of cystathionine-β-synthase (CBS) on colorectal cancer cell proliferation and bioenergetics in vitro. *Nitric Oxide* **41**, 146–156 (2014).

9. J. B. Vicente, *et al.*, NO* binds human cystathionine β-synthase quickly and tightly. *J. Biol. Chem.* **289**, 8579–8587 (2014).

10. M. R. Filipovic, J. Zivanovic, B. Alvarez, R. Banerjee, Chemical Biology of H2S Signaling through Persulfidation. *Chem. Rev.* **118**, 1253–1337 (2018).

11. M. D. Levitt, J. Furne, J. Springfield, F. Suarez, E. DeMaster, Detoxification of hydrogen sulfide and methanethiol in the cecal mucosa. *J. Clin. Invest.* **104**, 1107–14 (1999).

12. J. Furne, J. Springfield, T. Koenig, E. DeMaster, M. D. Levitt, Oxidation of hydrogen sulfide and methanethiol to thiosulfate by rat tissues: A specialized function of the colonic mucosa. *Biochem. Pharmacol.* **62**, 255–259 (2001).

13. F. Malagrinò, *et al.*, Hydrogen Sulfide Oxidation: Adaptive Changes in Mitochondria of SW480 Colorectal Cancer Cells upon Exposure to Hypoxia. *Oxid. Med. Cell. Longev.* **2019**, 8102936 (2019).

bioRxiv preprint doi: https://doi.org/10.1101/2020.03.06.979542; this version posted March 8, 2020. The copyright holder for this preprint (which was not certified by peer review) is the author/funder, who has granted bioRxiv a license to display the preprint in perpetuity. It is made available under aCC-BY-NC-ND 4.0 International license.

14. M. A. Kovach, *et al.*, Microarray analysis identifies IL-1 receptor type 2 as a novel candidate biomarker in patients with acute respiratory distress syndrome. *Respir. Res.* **16** (2015).

15. C. M. Mckinnon, H. Mellor, The tumor suppressor RhoBTB1 controls Golgi integrity and breast cancer cell invasion through METTL7B. *BMC Cancer* **17** (2017).

16. R. D. Thiagarajan, *et al.*, Identification of Anchor Genes during Kidney Development Defines Ontological Relationships, Molecular Subcompartments and Regulatory Pathways. *PLoS One* **6**, e17286 (2011).

17. D. Liu, *et al.*, METTL7B Is Required for Cancer Cell Proliferation and Tumorigenesis in Non-Small Cell Lung Cancer . *Front. Pharmacol.* **11**, 178 (2020).

18. P. C. Taylor, *et al.*, "Selective Inhibition of Janus Kinase 1 (JAK1) by Filgotinib Modulates the Disease-Associated Whole Blood Transcriptional Profile of Patients With Active Rheumatoid Arthritis."

19. A. Farnsworth, *et al.*, Acetaminophen Modulates the Transcriptional Response to Recombinant Interferon-ß. *PLoS One* **5**, e11031 (2010).

20. K. N. Kashkin, *et al.*, Genes potentially associated with Cisplatin resistance of lung cancer cells. *Dokl. Biochem. Biophys.* **438**, 147–150 (2011).

21. N. Ahmed, *et al.*, Unique proteome signature of post-chemotherapy ovarian cancer ascites-derived tumor cells. *Sci. Rep.* **6**, 30061 (2016).

22. M. Karaźniewicz-Łada, *et al.*, Clinical pharmacokinetics of clopidogrel and its metabolites

bioRxiv preprint doi: https://doi.org/10.1101/2020.03.06.979542; this version posted March 8, 2020. The copyright holder for this preprint (which was not certified by peer review) is the author/funder, who has granted bioRxiv a license to display the preprint in perpetuity. It is made available under aCC-BY-NC-ND 4.0 International license.

in patients with cardiovascular diseases. *Clin. Pharmacokinet.* **53**, 155–164 (2014).

23. J. Bremer, D. M. Greenberg, Enzymic methylation of foreign sulfhydryl compounds. *Biochim. Biophys. Acta* **46**, 217–224 (1961).

24. R. A. Keith, D. M. Otterness, A. L. Kerremans, R. M. Weinshilboum, S-Methylation of D- and L-penicillamine by human erythrocyte membrane thiol methyltransferase. *Drug Metab. Dispos.* **13**, 669–76 (1985).

25. C. Liu, *et al.*, Human liver cytochrome P450 enzymes and microsomal thiol methyltransferase are involved in the stereoselective formation and methylation of the pharmacologically active metabolite of clopidogrel. *Drug Metab. Dispos.* **43**, 1632–41 (2015).

26. M. Kazui, K. Hagihara, T. Izumi, T. Ikeda, A. Kurihara, Hepatic microsomal thiol methyltransferase is involved in stereoselective methylation of pharmacologically active metabolite of prasugrel. *Drug Metab. Dispos.* **42**, 1138–45 (2014).

27. R. S. Obach, C. Prakash, A. M. Kamel, Reduction and methylation of ziprasidone by glutathione, aldehyde oxidase, and thiol s-methyltransferase in humans: An in vitro study. *Xenobiotica* **42**, 1049–57 (2012).

28. R. A. Weisiger, W. B. Jakoby, Thiol S-methyltransferase from rat liver. *Arch. Biochem. Biophys.* **196**, 631–7 (1979).

29. T. A. Glauser, A. L. Kerremans, R. M. Weinshilboum, Human hepatic microsomal thiol methyltransferase. Assay conditions, biochemical properties, and correlation studies. *Drug*

bioRxiv preprint doi: https://doi.org/10.1101/2020.03.06.979542; this version posted March 8, 2020. The copyright holder for this preprint (which was not certified by peer review) is the author/funder, who has granted bioRxiv a license to display the preprint in perpetuity. It is made available under aCC-BY-NC-ND 4.0 International license.

Metab. Dispos. **20**, 247–55 (1992).

30. T. A. Glauser, E. Saks, V. M. Vasova, R. M. Weinshilboum, Human liver microsomal thiol methyltransferase: inhibition by arylalkylamines. *Xenobiotica* **23**, 657–69 (1993).

31. R. Borchardt, C. Cheng, Purification and Characterization of Rat Liver Microsomal Thiol Methyltransferase. *Biochim. Biophys. Acta* **522**, 340–353 (1978).

32. M. Käenmäki, *et al.*, Quantitative role of COMT in dopamine clearance in the prefrontal cortex of freely moving mice. *J. Neurochem.* **114**, 1745–1755 (2010).

33. J. Axelrod, Purification and Properties of Phenylethanolamine-N-methyl Transferase. *J. Biol. Chem.* **237**, 1657–1660 (1962).

34. D. D. Brown, J. Axelrod, R. Tomchick, Enzymatic N-Methylation of Histamine. *Nature* **183**, 680 (1959).

35. D. J. Thomas, S. B. Waters, M. Styblo, Elucidating the pathway for arsenic methylation. *Toxicol. Appl. Pharmacol.* **198**, 319–326 (2004).

36. P. K. Sahu, S. Chauhan, R. S. Tomar, The Crg1 N-Terminus Is Essential for Methyltransferase Activity and Cantharidin Resistance in Saccharomyces cerevisiae. *Biochemistry* **58**, 1799–1809 (2019).

37. R. M. Weinshilboum, S. L. Sladek, Mercaptopurine pharmacogenetics: Monogenic inheritance of erythrocyte thiopurine methyltransferase activity. *Am. J. Hum. Genet.* **32**, 651–662 (1980).

38. J. L. Wallace, J. G. P. Ferraz, M. N. Muscara, Hydrogen Sulfide: An Endogenous

bioRxiv preprint doi: https://doi.org/10.1101/2020.03.06.979542; this version posted March 8, 2020. The copyright holder for this preprint (which was not certified by peer review) is the author/funder, who has granted bioRxiv a license to display the preprint in perpetuity. It is made available under aCC-BY-NC-ND 4.0 International license.

Mediator of Resolution of Inflammation and Injury. *Antioxid. Redox Signal.* **17**, 58–67 (2011).

39. D. Wu, *et al.*, Hydrogen sulfide in cancer: Friend or foe? *Nitric Oxide* **50**, 38–45 (2015).

40. D. Wu, *et al.*, Hydrogen sulfide acts as a double-edged sword in human hepatocellular carcinoma cells through EGFR/ERK/MMP-2 and PTEN/AKT signaling pathways. *Sci. Rep.* **7** (2017).

41. K. J. Livak, T. D. Schmittgen, Analysis of Relative Gene Expression Data Using Real-Time Quantitative PCR and the 2−ΔΔCT Method. *Methods* **25**, 402–408 (2001).

42. X. Shen, *et al.*, Measurement of plasma hydrogen sulfide in vivo and in vitro. *Free Radic. Biol. Med.* **50**, 1021–31 (2011).

43. X. Shen, G. K. Kolluru, S. Yuan, C. G. Kevil, Measurement of H2S in vivo and in vitro by the monobromobimane method. *Methods Enzymol.* **554**, 31–45 (2015).

44. X. Shen, E. A. Peter, S. Bir, R. Wang, C. G. Kevil, Analytical measurement of discrete hydrogen sulfide pools in biological specimens. *Free Radic. Biol. Med.* **52**, 2276–2283 (2012).

45. A. Shevchenko, M. Wilm, O. Vorm, M. Mann, Mass Spectrometric Sequencing of Proteins from Silver-Stained Polyacrylamide Gels. *Anal. Chem.* **68**, 850–858 (1996).

bioRxiv preprint doi: https://doi.org/10.1101/2020.03.06.979542; this version posted March 8, 2020. The copyright holder for this preprint (which was not certified by peer review) is the author/funder, who has granted bioRxiv a license to display the preprint in perpetuity. It is made available under aCC-BY-NC-ND 4.0 International license.

Methods:

Materials: Mammalian overexpression plasmids and siRNA were purchased from Origene (Rockville, MD). HepG2 and HeLa cells were obtained from ATCC (Manassas, VA). Cell culture materials and lipofection reagents were purchased from ThermoFisher (Waltham, MA). Buffer salts were acquired from Sigma-Aldrich (St. Louis, MO) as well as methyltransferase probe substrates unless otherwise indicated. S-adenosyl-L-methionine and molecular biology kits were obtained from New England Biolabs (Ipswich, MA). Stellar Competent cells were purchased from Takara (Mountain View, CA). LOBSTR-BL21(DE3) competent cells were bought from Kerafast (Boston, MA). CHAPS detergent and UPLC-grade solvents were obtained from Fisher Scientific (Hampton, NH). Sequencing grade porcine trypsin and MTase-Glo Methyltransferase Assays were purchased from Promega (Madison, WI). 1,2-Dimyristoyl-*sn*-glycero-3-PG (DMPG) and mertansine were obtained from Cayman Chemical (Ann Arbor, MI). The active metabolite of prasugrel was a gift from Dr. Allan Rettie.

HepG2 and HeLa Cell Culture: Cells were maintained and expanded using Dubelco's Modified Eagle Medium supplemented with 10% fetal bovine serum and 0.1% penicillin/streptomycin. All cellular captopril methylation assays were conducted in serum-free media under optimized incubation conditions. Cells used for RNA isolation were washed with 1x phosphate buffered saline (PBS) prior to aspiration and storage at -80 ^{o}C until future use.

Gene Expression Modulation: HepG2 cells were treated with Lipofectamine RNAiMax (Thermo Fisher Scientific, Waltham, MA) according to the manufacturer protocol, optimized for transfection duration. *GAPDH* gene knockdown using the Trilencer small interfering RNA

bioRxiv preprint doi: https://doi.org/10.1101/2020.03.06.979542; this version posted March 8, 2020. The copyright holder for this preprint (which was not certified by peer review) is the author/funder, who has granted bioRxiv a license to display the preprint in perpetuity. It is made available under aCC-BY-NC-ND 4.0 International license.

(Origene, Rockville, MD) acted as the positive control for all gene expression knockdown experiments.

Cells were transfected in 12-well plates using a reverse transfection protocol. Briefly, *METTL7B* or scrambled siRNA was mixed with Lipofectamine RNAiMax in OptiMEM at room temperature for a final siRNA concentration of 50 nM. HepG2 cells were harvested using trypsin, pelleted, and resuspended to a final concentration of 200,000 cell/mL. Lipofectamine/siRNA stocks were added to culture plate wells, followed by 1 mL of cells, for a final concentration of 10 nM siRNA. Cells were allowed to incubate in the transfection media for 72 hours followed by RNA isolation or captopril methylation assays.

HeLa cells were treated with Lipofectamine 3000 (Thermo Fisher Scientific) according to the manufacturer protocol, optimized for transfection duration. Cells were transfected in 12-well plates via reverse transfection where purified empty or FLAG-tagged *METTL7B* overexpression plasmids (Origene) were mixed with P3000 reagent in OptiMEM at room temperature followed by Lipofectamine 3000. HeLa cells were harvested via trypsinization, pelleted, and resuspended to a final concentration of 200,000 cell/mL. Lipofectamine/plasmid stocks were added to culture plate wells, followed by 1 mL of cells, for a final plasmid concentration of 833 ng/mL. Cells were allowed to incubate in transfection media for 48 hours prior to RNA isolation or captopril methylation assays.

Measurement of Gene Expression Changes: Cellular RNA was extracted using the MagMAX 96 Total RNA Isolation kit (Thermo Fisher Scientific) according to the manufacturer protocol. RNA quality (A_{260}/A_{280}) and concentration was assayed using a NanoDrop spectrophotometer. Isolated RNA was used to create cDNA using the High Capacity RNA-to-

bioRxiv preprint doi: https://doi.org/10.1101/2020.03.06.979542; this version posted March 8, 2020. The copyright holder for this preprint (which was not certified by peer review) is the author/funder, who has granted bioRxiv a license to display the preprint in perpetuity. It is made available under aCC-BY-NC-ND 4.0 International license.

cDNA kit (Thermo Fisher Scientific) according to the manufacturer protocol. Subsequently, reverse-transcription polymerase chain reaction (RT-PCR) was conducted using an Applied Biosystems StepOnePlus Real-Time PCR System with TaqMan FAM reporter primers for *METTL7B*, *GAPDH*, and the housekeeping gene, *GusB*.

Expression level changes upon siRNA or plasmid treatment were determined using the $\Delta\Delta C_T$ method(41). In this method, *METTL7B* cycle threshold (C_t) values are normalized to *GusB* C_t values in all samples, yielding a ΔC_T value. Relative gene expression changes are then calculated between treated and control cells using $2^{-\Delta\Delta CT}$.

Cellular Captopril Methylation Assay: Cells with altered *METTL7B* gene expression were created as described above. After the appropriate transfection period, cells were washed with 1x PBS and treated with serum-free media containing 500 µM captopril. Cell media aliquots were sampled after 24 hours and the S-methyl captopril metabolite was measured via liquid chromatography-tandem mass spectrometry (LC/MS-MS) and multiple reaction monitoring (MRM).

The LC-MS/MS system used for captopril methylation analysis was a Waters Xevo TQS mass spectrometer paired with a Waters Acquity LC. Compound separation was achieved using a 2.1x100 mm Ascentis Express RP Amide column and 0.1% formic acid in water and 0.1% formic acid in methanol as solvents A and B respectively. Column temperature was maintained at 50 ^{o}C at all times. Chromatographic separation was obtained using the following gradient: solvent B was held at 30% from 0 to 3 min, then held at 90% from 3 to 7 min, followed by re-equilibration to the starting conditions for another 3 min for a total run time of 10 min. Flow rate

bioRxiv preprint doi: https://doi.org/10.1101/2020.03.06.979542; this version posted March 8, 2020. The copyright holder for this preprint (which was not certified by peer review) is the author/funder, who has granted bioRxiv a license to display the preprint in perpetuity. It is made available under aCC-BY-NC-ND 4.0 International license.

was held constant at 0.2 mL/min and flow was only diverted to the mass spectrometer between 2 to 7.5 min.

S-methyl captopril and the internal standard, d_3-*S*-methyl captopril, were monitored in positive mode. The monitored mass transitions m/z+ were 232.1 > 89 and 232.1 > 116 (S-methyl captopril) as well as 235.1 > 91.9 and 235.1 > 115.9 (internal standard). The MS conditions were as follows: collision energy 15 V, cone voltage 30 V, capillary voltage 3.2 kV, desolvation temperature 450 ^{o}C, desolvation gas flow 1,000 L/hr and cone gas 150 L/hr.

METTL7B Expression and Purification: Recombinant *METTL7B* was cloned in *E. coli* using a unique expression plasmid created in our lab. The expression plasmid backbone was obtained from pET21-10XHis-GST-HRV-dL5 which was a gift from Marcel Bruchez (Addgene plasmid # 73214; http://n2t.net/addgene:73214; RRID:Addgene_73214). The human *METTL7B* gene sequence was inserted into the plasmid using BamHI and EcoRI restriction sites and general molecular biology techniques. All plasmid inserts were sequenced by Eurofins Genomics and sequencing histograms were analyzed using FinchTV software.

Expression plasmids were propagated using heat-shocked Stellar cells. Individual colonies were used to create glycerol stocks and purify expression plasmids which were then sequenced for potential mutations. Validated plasmids were used to transform competent LOBSTR-BL21(DE3) *E. coli* via heat shock. Unless otherwise noted, all *E. coli* growth occurred on an orbital shaker at 250 rpm, 37 ^{o}C, and in the presence of 100 µg/mL ampicillin.

To express recombinant protein, LOBSTR-BL21(DE3) overnight cultures were added to ampicillin-containing TB expression media at a ratio of 1:100. Briefly, cells were grown for 3 hours under normal growth conditions. Then, METTL7B production was induced via addition

bioRxiv preprint doi: https://doi.org/10.1101/2020.03.06.979542; this version posted March 8, 2020. The copyright holder for this preprint (which was not certified by peer review) is the author/funder, who has granted bioRxiv a license to display the preprint in perpetuity. It is made available under aCC-BY-NC-ND 4.0 International license.

435 of isopropyl ß-D-1-thiogalactopyranoside (IPTG) to a final concentration of 1 mM. The
436 temperature was reduced to 15 ^{o}C and the cells were grown for an additional 24 hours. Cells
437 were harvested via gentle centrifugation and the collected pellets were stored at -80 ^{o}C until
438 future processing.

439 Frozen cell pellets were thawed on ice in a 4 ^{o}C cold cabinet overnight prior to
440 lysis. Lysis was conducted by resuspending the cell pellet in cell lysis buffer (50 mM KPi pH
441 7.0, 20% glycerol, 150 mM NaCl, 10 mM CHAPS, EDTA-free Halt Protease Inhibitor Cocktail)
442 supplemented with 100 µg/mL lysozyme (Sigma Aldrich). The cell solution was rotated end-
443 over-end at 4 ^{o}C until the solution had become extremely viscous. Then, the cell lysate was
444 treated with 100 µg/mL DNA Nuclease I (Sigma Aldrich) and rotated at 4 ^{o}C or until no longer
445 viscous. The lysate was then centrifuged at 48,000 g for 30 minutes at 4 ^{o}C and the resulting
446 supernatant was retained for subsequent purification steps.

447 Purification was conducted using the ÄKTA start chromatography system (GE
448 Healthcare). Cell lysate supernatant was applied to a pre-packed and conditioned HisPur Ni-
449 NTA column (ThermoFisher) overnight at a low flow rate (0.5 mL/min). The column was
450 subsequently washed with Ni-NTA purification buffer (50 mM KPi pH 7.0, 20% glycerol, 10
451 mM CHAPS, 300 mM NaCl) containing 50 mM imidazole until A_{280} readings stabilize. Protein
452 was eluted from the column with purification buffer containing 300 mM imidazole until A_{280}
453 readings stabilized.

454 The HisPur Ni-NTA column eluent was directly applied to a pre-conditioned GSTrapFF
455 column at a flow rate of 1 mL/min for 4 hours. The column was then washed with GSTrapFF
456 purification buffer (50 mM KPi pH 7.0, 20% glycerol, 10 mM CHAPS, 150 mM NaCl) until

bioRxiv preprint doi: https://doi.org/10.1101/2020.03.06.979542; this version posted March 8, 2020. The copyright holder for this preprint (which was not certified by peer review) is the author/funder, who has granted bioRxiv a license to display the preprint in perpetuity. It is made available under aCC-BY-NC-ND 4.0 International license.

457 A_{280} had decreased to baseline. Recombinant protein was eluted from the column using
458 purification buffer containing 10 mM reduced glutathione and adjusted to pH 8.0. Pooled eluent
459 was concentrated to appropriate working concentrations using Amicon Centriprep 10K
460 molecular weight cutoff centrifugal filter units. Final protein concentration was determined by
461 A_{280} measurement and stocks were aliquoted and stored at -80 ^{o}C until future use.

462 *In vitro Captopril Methylation Using Recombinant METTL7B: In vitro* captopril methylation
463 was conducted using purified METTL7B fusion protein. The reaction buffer (50 mM KPi pH
464 7.0, 10 mM CHAPS, 20% glycerol, 150 mM NaCl, and 9 mg/mL DMPG) was placed in a
465 sonication water bath until the solution was clear to help form DMPG liposomes. Recombinant
466 enzyme was added at a ratio of 85:1 DMPG:METTL7B and allowed to incubate on ice for 30
467 minutes. Following the addition of captopril, the enzyme was pre-equilibrated at 37 ^{o}C for 2
468 minutes before initiation by addition of SAM to a reaction volume of 150 µL. The final
469 concentration of captopril was varied to collect the kinetic information and the final
470 concentration of SAM was held at 750 µM. The reaction was incubated for 25 minutes and then
471 quenched via addition of 15% (w/v) zinc sulfate in a 1:5 dilution to total reaction volume. The
472 quenched solution was incubated on ice for 10 minutes followed by a 1:6 addition of a saturated
473 barium hydroxide solution containing the d_3-S-methyl captopril internal standard. Following a
474 second 10-minute incubation on ice, the solution was centrifuged at 5,000 xg for 15 minutes to
475 pellet all precipitated proteins and salts.

476 Following centrifugation, 75 µL of supernatant was transferred to an opaque
477 polypropylene strip-well tube containing 5 µL of 2 M sodium hydroxide. Unreacted captopril
478 was derivatized at room temperature for 1 hour in the dark via addition of 20 µL of 2.5 M

bioRxiv preprint doi: https://doi.org/10.1101/2020.03.06.979542; this version posted March 8, 2020. The copyright holder for this preprint (which was not certified by peer review) is the author/funder, who has granted bioRxiv a license to display the preprint in perpetuity. It is made available under aCC-BY-NC-ND 4.0 International license.

maleimide to reduce ion suppression from non-methylated captopril. Derivatized samples were centrifuged and the supernatant was analyzed by LC-MS/MS as previously described.

In vitro Hydrogen Sulfide Methylation Using Recombinant METTL7B: Protein concentration and incubation with DMPG liposomes was conducted the same as described above. All steps were conducted in a glove box under nitrogen unless otherwise indicated. Recombinant enzyme was aliquoted into a polypropylene deep-well plate on ice along with SAM and NaSH for a final volume of 150 µL and 0.09 mg/mL and 83.3 µM for protein and SAM concentrations respectively. The plate was capped with a silicon mat and placed in a 37 ^{o}C water bath for 45 min under normal atmosphere. After incubation, the plate was placed back on ice under nitrogen and quenched via a 1:15 addition of 0.3 M sodium hydroxide. 110 µL of the quenched reaction solution was added to 50 µL of 20 mM monobromobimane (MBB), based off of published H_2S derivatization method(42–44). Once capped under nitrogen, the reaction plate was incubated at room temperature on an orbital shaker at 450 rpm for 30 min.

The MBB derivatization was quenched by addition of 50 µL of 200 mM 5-sulfosalicylic acid and 10 µL of the ethyl 2-aminothiazole carboxylate (EATC) internal standard. Protein was precipitated by addition of 15% (w/v) zinc sulfate and barium hydroxide as previously detailed. Samples were centrifuged at 4,000 xg for 15 min and the supernatant was analyzed by LC-MS/MS.

The LC-MS/MS system used for hydrogen sulfide methylation analysis was a Waters Xevo TQS mass spectrometer paired with a Waters Acquity LC. Compound separation was achieved using a 2.1x150 mm Acquity UPLC BEH Shield RP column and 0.2% acetic acid in water and 0.2% acetic acid in acetonitrile as solvents A and B respectively. Column temperature

bioRxiv preprint doi: https://doi.org/10.1101/2020.03.06.979542; this version posted March 8, 2020. The copyright holder for this preprint (which was not certified by peer review) is the author/funder, who has granted bioRxiv a license to display the preprint in perpetuity. It is made available under aCC-BY-NC-ND 4.0 International license.

was maintained at 25 ^{o}C at all times. Chromatographic separation was obtained using the following gradient: solvent B was held at 40% from 0 to 1 minutes, ramped to 90% from 1 to 3.5 minutes, held at 90% from 4.5 to 5 minutes followed by re-equilibration to the starting conditions for another minute. Flow rate was held constant at 0.3 mL/min and flow was only diverted to the mass spectrometer from 1 to 4.5 minutes.

Derivatized methanethiol and the internal standard, EATC, were monitored in positive mode. The monitored mass transitions m/z+ were 239.22 > 175.24 and 239.22 > 192.2 (derivatized methanethiol) as well as 173.17 > 72.11 and 173.17 > 127.06 (internal standard). The MS conditions were as follows: collision energy 24, 10, 24, 16 V for each transition respectively, cone voltage 56 V, capillary voltage 2.9 kV, desolvation temperature 450 ^{o}C, desolvation gas flow 1,000 L/hr and cone gas 150 L/hr.

Protein Purity Analysis: All SDS-PAGE silver stain analysis was conducted using NuPAGE 4-12% Bis-Tris gels in the XCell SureLock Mini-Cell Electrophoresis system using PageRuler Plus Prestained Protein Ladder as a molecular weight marker. Samples were prepared using NuPAGE LDS Sample Buffer sample buffer and 1.4 M ß-mercaptoethanol before boiling for 5 minutes. Gels were run at room temperature, at a constant 200 volts, and developed using previously published silver staining protocols(45).

All western blot analyses were conducted using the XCell SureLock Mini-Cell Electrophoresis system, PageRuler Plus Prestained Protein Ladder, and NuPAGE 10-20% Tricine gels. Samples were prepared using 4X Protein Loading Buffer (LiCor) and 0.7 M ß-mercaptoethanol before boiling for 5 minutes. After initial SDS-PAGE separation, the gel was removed from the cassette and placed with PVDF blotting membrane into the XCell II Blot

bioRxiv preprint doi: https://doi.org/10.1101/2020.03.06.979542; this version posted March 8, 2020. The copyright holder for this preprint (which was not certified by peer review) is the author/funder, who has granted bioRxiv a license to display the preprint in perpetuity. It is made available under aCC-BY-NC-ND 4.0 International license.

Module according to the manufacturer protocol. Blot transfer was conducted over 1 hour at a constant 30 volts on ice. The blot was blocked using Odyssey Blocking Buffer (LiCor) for 1 hour at room temperature. A primary antibody incubation was conducted overnight using the suggested dilution factor for the rabbit anti-METTL7B (Sigma Aldrich), anti-FLAG (Cell Signaling), anti-GST (Cell Signaling), or anti-ß actin (Cell Signaling) antibodies. The secondary antibody incubation was conducted for 1 hour at room temperature using IRDye 680RD goat anti-rabbit antibody (LiCor). Western blots were scanned using an Odyssey gel scanner. Blot images were visualized using Image Studio Version 4.0 software.

Tryptic Digest: In-gel tryptic digests of silver stained SDS-PAGE gels were conducted following the method published by Shevchenko(45). Briefly, the protein band was excised from the gel and dehydrated with neat acetonitrile. Protein bands were then treated with 10 mM dithiothreitol (DTT) solution and incubated at 56 ^{o}C to reduce all proteins. The reduced bands were treated with 55 mM iodoacetamide at room temperature in the dark to alkylate all exposed cysteine side chains. Finally, the bands were incubated overnight at 37 ^{o}C with 13 ng/µL trypsin-containing solution. Tryptic digestion peptides were extracted from the gel bands the following day and concentrated in a centrifugal evaporator. Concentrated peptides were analyzed using a high-resolution mass spectrometer, a Finnigan LTQ Orbitrap in our case, and then used to identify the protein of interest via ProteinProspector.

The LC-MS system used for proteomic analysis was a Finnigan LTQ Orbitrap coupled to a Waters Acquity LC. Peptides were separated using a 1x150 mm Acquity UPLC CSH C18 column and 0.1% formic acid in water and 0.1% formic acid in acetonitrile as solvents A and B. Separation was achieved using the following gradient: solvent B was held at 5% for the first two minutes, increased to 40% over the next 90 min, increased to 90% over the next five minutes and

bioRxiv preprint doi: https://doi.org/10.1101/2020.03.06.979542; this version posted March 8, 2020. The copyright holder for this preprint (which was not certified by peer review) is the author/funder, who has granted bioRxiv a license to display the preprint in perpetuity. It is made available under aCC-BY-NC-ND 4.0 International license.

held for an additional 8 minutes, then re-equilibrated over five minutes. The flow rate was held at 0.06 mL/min and flow as diverted to the mass spectrometer from 2 to 95 minutes.

Peptides were analyzed using a data dependent scan method in positive mode. The initial high resolution scan from 300-2,000 m/z was conducted in the FTMS with 60,000 resolution. Four dependent scans were completed in the ion trap to obtain fragmentation. Dynamic exclusion was enabled which excluded the top 25 most intense ions after they had been selected twice over a four second window. The following mass spectrometer settings were used: sheath gas flow rate was 12 arb, spray voltage was 3.5 kV, capillary temperature was 350 ^{o}C, capillary voltage was 22 V, and tube lens voltage was 100 V.

Substrate Screening: Substrate screening was primarily conducted using the MTase-Glo Assay (Promega). Briefly, recombinant METTL7B was prepared the same way as for use in the captopril methylation assay. SAM was added to the METTL7B protein stock for a final concentration of 50 µM and was aliquoted into a 384-well plate. Substrate was added to each well and the plate was covered using Parafilm before incubating at 37 ^{o}C for 1 hour. The incubation was quenched by a 1:5 addition of 0.5% trifluoro acetic acid. The samples were processed according to the manufacturer protocol and luminescence was recorded for each well using a Synergy HTX Multi-Mode Reader (BioTek).

Data Analysis: All experiments were conducted with biological triplicates, and repeated at least two times on two different days. All data is reported as the mean ± standard deviation, however individual data points from multiple experiments are presented when possible. Statistical significance was determined by a two-tailed unpaired *t* test with a threshold *P* value of 0.05.

bioRxiv preprint doi: https://doi.org/10.1101/2020.03.06.979542; this version posted March 8, 2020. The copyright holder for this preprint (which was not certified by peer review) is the author/funder, who has granted bioRxiv a license to display the preprint in perpetuity. It is made available under aCC-BY-NC-ND 4.0 International license.

Kinetic parameter Km values were obtained through non-linear regression analysis using GraphPad Prism, version 8.3.1 for Windows (GraphPad Software, La Jolla, CA).

Data Availability Statement: The proteomic data that support the findings of this study are available from PeptideAtlas, tagged as "pET21METTL7B". All other data are available from the corresponding author upon reasonable request.

Materials Availability Statement: Unique materials used when conducting the experiments detailed in this study are available from the corresponding author upon reasonable request.

Competing Interest Declaration: All authors declare no competing interests.

Funding Statement: This work was partially funded by the National Institute of Health Heart Lung and Blood institute grant number R01HL146603. BM was supported in part by the National Institute of General Medical Sciences of the National Institutes of Health under Award Number T32GM 007750 and the National Center For Advancing Translational Sciences of the National Institutes of Health under Award Number TL1 TR002318. The content is solely the responsibility of the authors and does not necessarily represent the official views of the National Institutes of Health